

# Topological Properties of the QCD Vacuum at $T = 0$ and $T \sim T_c$

Philippe de Forcrand <sup>1</sup>, Margarita García Pérez <sup>2</sup>, James E. Hetrick <sup>3</sup>,  
Ion-Olimpiu Stamatescu <sup>4</sup>

<sup>1</sup> SCSC, ETH-Zürich, CH-8092 Zürich, Switzerland

<sup>2</sup> Theory Division, CERN, CH-1211, Geneve 23, Switzerland

<sup>3</sup> Physics Dept., University of the Pacific, Stockton, CA 95211-0197, USA

<sup>4</sup> FESst, Schmeilweg 5, D-69118, Heidelberg

and

Institut für Theoretische Physik, Philosophenweg 16, D-69120, Heidelberg, Germany

**Abstract:** We study on the lattice the topology of  $SU(2)$  and  $SU(3)$  Yang-Mills theories at zero temperature and of  $QCD$  at temperatures around the phase transition. To smooth out dislocations and the UV noise we cool the configurations with an action which has scale invariant instanton solutions for instanton size above  $\sim 2.3$  lattice spacings. The corresponding “improved” topological charge stabilizes at an integer value after few cooling sweeps. At zero temperature the susceptibility calculated from this charge (about  $(195 \text{ MeV})^4$  for  $SU(2)$  and  $(185 \text{ MeV})^4$  for  $SU(3)$ ) agrees very well with the phenomenological expectation. At the minimal amount of cooling necessary to resolve the structure in terms of instantons and anti-instantons we observe a dense ensemble where the total number of peaks is by a factor 5-10 larger than the net charge. The average size observed for these peaks at zero temperature is about 0.4-0.45 fm for  $SU(2)$  and 0.5-0.6 fm for  $SU(3)$ . The size distribution changes very little with further cooling, although in this process up to 90% of the peaks disappear by pair annihilation. For  $QCD$  we observe below  $T_c$  a drastic reduction of the topological susceptibility as an effect of the dynamical fermions. Nevertheless also here the instantons form a dense ensemble with general characteristics similar to those of the quenched theory. A further drop in the susceptibility above  $T_c$  is also in rough agreement with what has been observed for pure  $SU(3)$ . We see no clear signal for dominant formation of instanton - anti-instanton molecules.

## 1 Introduction

The vacuum of the 4-dimensional  $SU(N_c)$  gauge theories has a non-trivial topological structure generated by different coverings of the spatial sphere at  $\infty$  with gauge transformations from the  $SU(2)$  subgroups. The tunneling field configurations between these different vacua, the instantons, are self-dual solutions of the classical, euclidean equations of motion of finite euclidean action and integer topological charge:  $S_0 = \int d^4x s(x) = 8\pi^2$ ,  $Q_0 = \int d^4x q(x) = \pm 1$ . The so called ‘t Hooft ansatz

$$s(x) = F^2(x) = \frac{48}{\rho^4} \left[ 1 + \sum_{\mu=1}^4 \left( \frac{x_\mu - x_\mu^0}{\rho} \right)^2 \right]^{-4}, \quad q(x) = \frac{Q_0}{8\pi^2} s(x) \quad (1)$$

describes an isolated instanton of size  $\rho$ , centered at  $x^0$ . Obviously these are scale invariant solutions. Superpositions of  $N$  instantons or anti-instantons also corresponds to (higher) minima of the action:

$S = NS_0$ , however a pair instanton - anti-instanton is not a minimum and its total action depends, among other, by the amount of “overlap”  $\omega = \rho_I \rho_A / |x_I^0 - x_A^0|^2$ .

Effects associated with instantons are:

1.  $U_A(1)$  *symmetry breaking*. This effect is succinctly described by the Witten - Veneziano formula[1] relating the topological susceptibility  $\chi$  and the  $\eta'$  mass:

$$\chi \equiv \lim_{V \rightarrow \infty} \frac{1}{V} \int dx^4 \langle T(q(x)q(0)) \rangle = \frac{f_\pi}{2N_f} (m_\eta^2 + m_{\eta'}^2 - 2m_K^2). \quad (2)$$

Here  $\chi$  has to be obtained in a quenched simulation. Since the instantons are essentially an  $SU(2)$  phenomenon, the result should not depend strongly on  $N_c$ . The empirical data for the RHS of (2) give  $\chi = (180\text{MeV})^4$ . Notice that the presence of light fermions inhibits the topological susceptibility (the Dirac operator for massless fermions has zero modes for  $Q \neq 0$ ).

2. *Chiral symmetry breaking*. By inducing zero modes of the Dirac operator instantons may control the chiral symmetry breaking, due to the Banks-Casher relation  $\langle \psi\bar{\psi} \rangle = \frac{1}{\pi} \langle \rho(0) \rangle$  in which  $\rho(\lambda)$  is the spectral density of the Dirac operator. Spontaneous symmetry breaking then results from a nonzero density of eigenvalues at  $\lambda = 0$ .

3. *Dynamical effects*. Instantons are believed to influence the dynamics of the intermediate distances (at the scale of  $\frac{1}{2}$  fm, say) and therefore the hadron properties. Their infrared effects are, however, less certain, in particular there is an open question whether they lead to confinement.

The  $U_A(1)$  symmetry breaking involves only the integrated correlation  $\chi$ . This can be tested directly in numerical simulations. The effects in 2. and 3. depend on details of the instanton population. Predictions can be made with help of models. Numerical simulations are then asked to test the ingredients on which these models are based. The features relevant for our discussion are:

(i) The instantons can be in a gas, liquid, or crystalline phase depending on their density and overlap. The diluteness of the ensemble is expressed by the “packing fraction”  $f = \pi^2/2 \langle \rho^4 \rangle N/V$ .

(ii) The size distribution controls the diluteness and the I-R properties. In the dilute gas approximation the estimation of the fluctuation determinant [2] permits to predict a power law for small sizes. In case of a dense population of instantons, by just integrating in a finite volume and assuming convergence of the thermodynamic limit one can derive some rather general features of the size distribution [3]. This leads to a different power law behavior for the small size distribution. We can write:

$$P(\rho) \sim \rho^p, \quad p_{dilute} = -5 + b, \quad p_{dense} = -1 + 4(b-4)/b, \quad b = 11N_c/3 \quad (3)$$

(iii) Denoting by  $N_I(N_A)$  the number of instantons (anti-instantons) in a configuration, and with  $N = N_I + N_A$ , we write:

$$c \equiv (\langle N^2 \rangle - \langle N \rangle^2) / \langle N \rangle. \quad (4)$$

The quantity  $c$  tests the Poisson character of the  $N$  - distribution. For a poissonian distribution  $c = 1$ , while low energy sum rules [4] suggest  $c = \frac{4}{b}$ .

(iv) In the “standard” model [5] the QCD instanton ensemble below the critical temperature is an interacting instanton liquid with density about  $N/V = 1 \text{ fm}^{-4}$ . The instanton size distribution has an infrared cut-off and an average instanton size of  $\sim 1/3$  fm. The dynamics of the chiral phase transition is driven by a rearrangement of the instanton ensemble at  $T_c$  - I-A molecules are formed, with a tendency to orientation along the euclidean time axis (this effect is due to light fermions).

## 2 Method

Topology analyses for lattice regularized fields have the usual two sources of systematic errors: cut-off effects and finite size effects. Short range topological fluctuations, at the level of the cut-off, are unphysical. They typically have an action lower than  $S_0$  (dislocations) and can spoil the determination of the susceptibility and distort the properties of the instanton ensemble. The finite size of the lattice, on

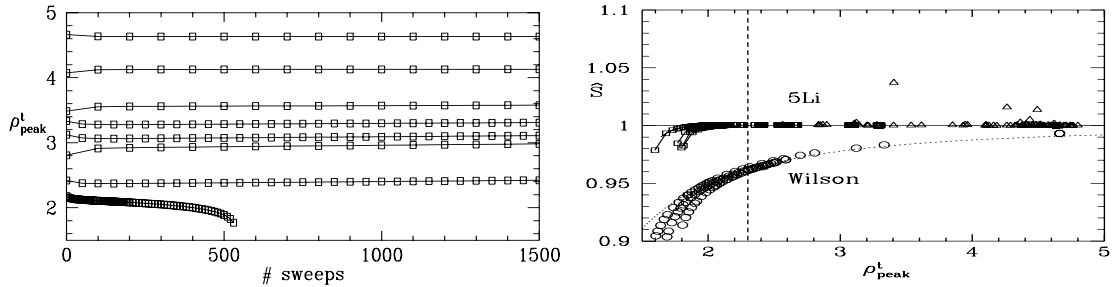


Figure 1: Evolution of the size of instantons under improved cooling (left) and the (improved: 5Li or Wilson) action of instantons of various sizes (right). For the determination of  $\rho_{\text{peak}}$  see [6].

the other hand, distorts the properties of the ensemble at sizes beyond  $l/2$  ( $l$ : the physical lattice size). To cope with this latter problem we must use a large enough lattice compared with the range of distances we are interested in and check the dependence on the boundary conditions. The short distance problem is more involved. The method we have adopted for obtaining sensible densities is to cool the Monte Carlo configurations to smooth out the UV-noise, and in particular to eliminate the dislocations. However, the usual plaquette action has, strictly speaking, no instanton solutions since for them the action is always smaller than  $S_0$  and becomes lower with decreasing size. Under Wilson cooling the instantons therefore shrink and after some time disappear. We have used instead an improved action which has true, scale invariant instanton solutions for sizes  $\rho > \rho_0$  with a threshold  $\rho_0 \simeq 2.3a$  – see Fig. 1. This action involves 5 Wilson loops and a similar construction yields an improved charge operator which is practically an integer already on rather rough configurations [6].

Cooling proceeds by local minimization of the action and leads to the global minimum, which is determined by the topological sector  $Q$ . From the point of view of our analysis it has two effects. On the one hand it smoothes out the short distance fluctuations, including dislocations and makes apparent the physical distance structure. On the other hand it annihilates I - A pairs depending on the overlap between the opposite charges.

Since the (improved) charge operator  $Q$  stabilizes to an integer value within 1 - 2% already after very few cooling sweeps (5 - 10) the effects of type 1. above are well defined in our method without further tuning, monitoring, etc. The susceptibility and charge distributions show good scaling behavior which implies that they reveal a physical structure. The ensemble properties, on the other hand will depend, at least in part, on the degree of cooling. This affects the discussion of points 2. and 3. above and the corresponding tests for instanton models.

### 3 Analysis

We have analyzed the  $SU(2)$  and  $SU(3)$  Yang-Mills theories at  $T = 0$ . We varied the cut-off and the lattice size such as to have the same physical volume at different discretization scales. For the  $SU(2)$  analysis we used twisted boundary conditions [6]. We have studied  $QCD$  with two flavors of staggered fermions of mass  $ma = 0.008$  at 3 temperatures around  $T_c$  on configurations kindly provided to us by the MILC collaboration. The lattices and the main results are given in Table 3.

#### TOPOLOGICAL SUSCEPTIBILITY

As can be seen from the Fig. 2 the  $T = 0$  topological susceptibility is practically independent of cooling and scales correctly.  $\chi^{1/4}$  shows a value of 195 – 200 MeV for  $SU(2)$  and 180 – 185 MeV for  $SU(3)$  with a typical error of about 5%, in very good agreement with experiment following (2) – see also Table 3. This coincides with the results obtained using improved operators [8], underrelaxed Wilson cooling [9], constrained smearing [10] and with the fermionic overlap formalism [11] (where the charge density itself has been tested). The results of [12] are about 10% higher, still compatible with (2) inside 2 standard

Table 1: Lattices and cooling results

Lattice	Sw.	$\langle N \rangle$	$c$	$\langle N \rangle / fm^4$
<b>(1)</b> $SU(2), \beta = 2.4$ $a = 0.12 fm$ $12^4, 217 conf.$	20	10.4	0.4	2.4
	50	5.0	0.5	1.2
	150	2.45	0.7	0.6
	300	2.12	1.0	0.5
<b>(2)</b> $SU(2), \beta = 2.6$ $a = 0.06 fm$ $24^4, 115 conf.$	20	63.0	0.6	14.
	50	15.6	0.65	3.6
	150	6.5	0.65	1.5
	300	3.8	0.5	0.9
<b>(3)</b> $SU(3), \beta = 5.85$ $a = 0.134 fm$ $12^4, 120 conf.$	20	12.10	0.36	1.81
	50	5.93	0.5	0.89
	150	2.52	1.0	0.38
<b>(4)</b> $SU(3), \beta = 6.0$ $a = 0.1 fm$ $16^4, 120 conf.$	20	21.63	0.5	3.30
	50	9.38	0.5	1.43
	100	5.33	0.5	0.81
<b>(5)</b> $QCD, \beta = 5.65$ $a = 0.115 fm$ $24^3 12, 31 conf.$	20	50.68	0.41	1.75
	50	14.90	1.	0.51
	100	7.77	0.8	0.27
	150	5.68	1.	0.20
<b>(6)</b> $QCD, \beta = 5.725$ $a = 0.103 fm$ $24^3 12, 43 conf.$	20	42.95	0.57	2.30
	50	8.86	0.82	0.47
	100	2.81	0.98	0.15
	150	1.84	1.03	0.10
<b>(7)</b> $QCD, \beta = 5.85$ $a = 0.0855 fm$ $24^3 12, 20 conf.$	20	35.0	0.4	3.95
	50	5.55	0.84	0.63
	100	0.50	0.9	0.06

deviations (see [13] for a possible explanation). We can conclude therefore that at present the  $T = 0$  topological susceptibility is under control and in good agreement with the Witten-Venetiano formula.

Table 2: Average charge and topological susceptibility

Lattice	<b>(1)</b>	<b>(2)</b>	<b>(3)</b>	<b>(4)</b>	<b>(5)</b>	<b>(6)</b>	<b>(7)</b>
$\langle  Q  \rangle$	1.6(1)	1.5(2)	1.8(2)	1.7(2)	2.0(4)	0.9(1)	0
$\chi^{1/4}$ MeV	195(4)	194(14)	184(6)	182(7)	134(10)	102(5)	0

The finite temperature deconfining transition of the pure Yang-Mills theory has been shown to produce a strong drop in the susceptibility [8, 10]. We have analyzed here the finite temperature QCD. Below  $T_c$  we found as expected a reduction in the susceptibility (by a factor 3), indicative of the dynamical fermion effects. Above  $T_c$  (which is at  $\sim 160 MeV$  for the MILC simulation) we found a pronounced drop in  $\chi$ , similar to the quenched case. As already observed before for other staggered fermion simulations [14] also the MILC configurations show long range correlations in  $Q$  and explore few topological sectors. The results quoted in Table 3 are obtained after symmetrizing per hand the charge distribution (since this is a symmetry of the action), the errors given are only the statistical ones. We have noticed such metastabilities also in the pure  $SU(3)$  simulation, there, however, one can afford to wait until the

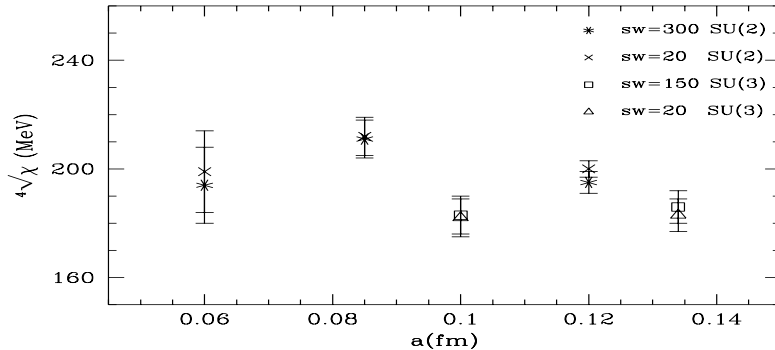


Figure 2: Topological susceptibility for quenched  $SU(2)$  and  $SU(3)$ .

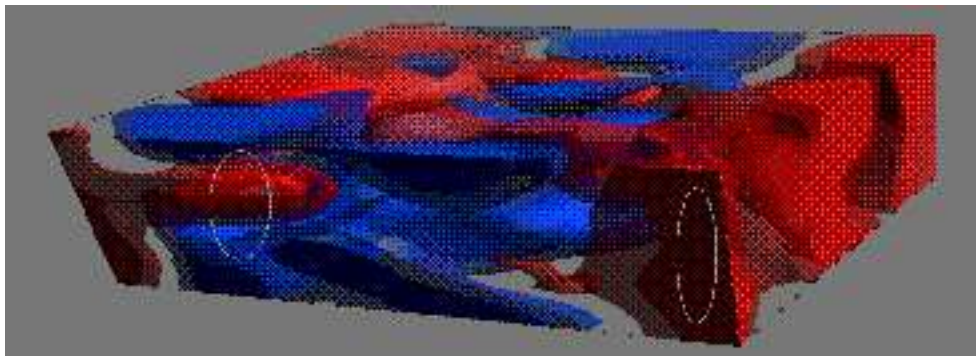


Figure 3: Isosurfaces for the charge density of a typical configuration of lattice (6), Table 1., after 20 sweeps of improved cooling; the two circles indicate a “molecule” (left) and a “caloron” (right).

configurations decorrelate.

### THE INSTANTON ENSEMBLE

To observe not merely the global charge of a configuration but its structure describable in terms of instantons and anti-instantons a certain degree of smoothing must be attained (see Fig. 3 for an illustration). Using our improved cooling we achieve this smoothness with a number of cooling sweeps between 20 and 50, depending on the cut-off  $a$ . We did not try to tune a rescaling law for the amount of cooling [9], since for many of the results this was not necessary due to inherent stability properties of our cooling.

As can be seen from the tables, when the configurations are just smooth enough for us to see instantons and anti-instantons we typically have a ratio  $N/|Q| \simeq 6 - 10$ . This ratio is reduced to  $N/|Q| \simeq 1 - 2$  in the further cooling by pair annihilation, leaving only the (anti-)instantons corresponding to the topological sector. The first remark is that the size distribution shows only little variation during this process – see Fig. 4 for the quenched simulation. This implies that all the (anti-)instantons which we observe from the start obey the same distribution. The average sizes are in the region of 0.4fm for  $SU(2)$  and 0.6fm for  $SU(3)$  and  $QCD$ . The small size part of the distribution departs from the dilute gas power law and shows tendency toward agreement with [3, 15] ( $p \simeq 0.8$  for  $SU(2)$  and 1.5 for  $SU(3)$  – compare eq. (3)).

The density of (anti-)instantons is high to start with. Because of this high density and of the rather large sizes, the packing fraction here is also high. The overall distribution is here non-poissonian and in agreement with the low energy sum rules, see eq. (4) and Table 3 (while it approaches the poissonian distribution for instantons *or* anti-instantons after long cooling). This suggests a dense ensemble with a spatially random distribution biased toward small  $|Q|$ . Similar results at  $T = 0$  have been reported in [9].

To the extent we could follow the structure described by this ensemble back to shorter cooling, it does not change in character but becomes more and more obscured by the accumulation of short range ripples

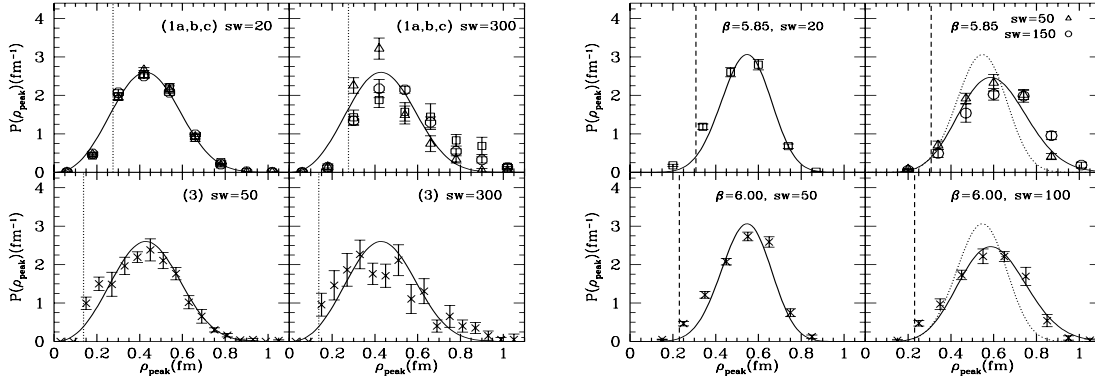


Figure 4: Size distributions for quenched  $SU(2)$  (left) and  $SU(3)$  (right).

and dislocations. This corroborates with the stability of distributions under further cooling (Fig. 4) and their correct scaling behavior to suggest the physical relevance of this ensemble. Since the short cooling needed before we can observe the instantons and anti-instantons might have also annihilated some pairs in the physically relevant size region, the figures we obtain for the density of (anti-)instantons are lower bounds.

For  $QCD$  at high  $T$  molecule formation with preferred orientation should be revealed by an anisotropy in the density - density correlations along space and along (euclidean) time directions. The anisotropy we observe at very short cooling is compatible with zero at the level of two standard deviations and very low in relative value (compared to the correlation itself) [7]. This signal is too weak to support the scenario of [5], however the quark mass might not be yet small enough to promote a strong effect. See also Fig. 3.

We conclude that we observe a dense ensemble randomly distributed in space, but with a bias toward small  $|Q|$ . This ensemble is revealed after a short cooling which essentially has filtered out dislocations and strongly overlapping IA pairs. We remark as a question of principle that any separation

$$q(x) = \text{instantons} + \text{trivial fluctuations}$$

is inherently ambiguous in the case of such strongly overlapping pairs. It is therefore not clear to us whether this latter structure is reasonably described as instantons and anti-instantons or a description in terms of other kind of excitations is more suitable for it.

**ACKNOWLEDGMENTS:** We wish to thank D. Diakonov, A. Di Giacomo, T. De Grand, A. Hasenfratz, M. Ilgenfritz, M. Mueller-Preussker, G. Münster, R. Narayanan and T. Kovács for discussions. MGP and IOS thankfully acknowledge partial support from the DFG.

## References

- [1] E. Witten, Nucl. Phys. B156 (1979) 269; G. Veneziano, Nucl. Phys. B159 (1979) 213.
- [2] G. 't Hooft, Phys. Rev. Lett.37 (1976) 8; Phys. Rev. D14 (1976) 3432.
- [3] G. Münster, Z. Phys. C, Particles and Fields 12 (1982) 43.
- [4] E.-M. Ilgenfritz and M. Mueller-Preussker, Phys. Lett. B99 (1981) 128; D. Diakonov and V. Petrov, Nucl. Phys. B245 (1984) 259.
- [5] for a review see T. Schäfer and E.V. Shuryak, hep-ph/9610451.
- [6] Ph. de Forcrand, M. García Pérez and I.-O. Stamatescu , Nucl. Phys. B (Proc. Suppl.) 47 (1996) 777; Nucl. Phys. B499 (1997) 409.

- [7] Ph. de Forcrand, M. García Pérez, J.E. Hetrick and I.-O. Stamatescu, hep-lat/9710001.
- [8] B. Allés, M. D'Elia and A. Di Giacomo, Nucl. Phys. B494 (1997) 281.
- [9] D. A. Smith and M. J. Teper, hep-lat/9801008.
- [10] M. Feuerstein, E.-M. Ilgenfritz, M. Müller-Preussker and S. Thurner, hep-lat/9611024.
- [11] R. Narayanan and P. Vranas, Nucl. Phys. B506 (1997) 373.
- [12] T. De Grand, A. Hasenfratz and T. Kovács, hep-lat/9705009, hep-lat/9711032.
- [13] R. Narayanan and R. L. Singleton Jr., hep-lat/9709014.
- [14] B. Allés, G. Boyd, M. D'Elia, A. Di Giacomo and E. Vicari, hep-lat/9607049.
- [15] Ph. De Forcrand, M. García Pérez, J. Hetrick, G. Münster and I.-O. Stamatescu, in preparation.